DALTON
FULL PAPER

Electropolymerisable bipyridine ruthenium(II) complexes. Synthesis and electrochemical characterisation of 4-(3-methoxystyryl)- and 4,4′-di(3-methoxystyryl)-2,2′-bipyridine ruthenium complexes

Viviane Aranyos,[ab] **Johan Hjelm,**[b] **Anders Hagfeldt**[b] **and Helena Grennberg** *[a]

[a] *Department of Organic Chemistry, University of Uppsala, Box 531, S-751 21, Uppsala, Sweden. E-mail: helenag@kemi.uu.se*
[b] *Department of Physical Chemistry, University of Uppsala, Box 532, S-751 21, Uppsala, Sweden*

Received 30th October 2000, Accepted 14th February 2001
First published as an Advance Article on the web 28th March 2001

A number of new ruthenium polypyridyl complexes with mono- or di-(3-methoxystyryl) substituted bipyridines have been synthesized. The complexes were characterised by NMR, elemental analysis, UV-vis absorption and emission spectroscopy, and cyclic voltammetry. Electroactive polymer films of these complexes have been prepared both by oxidative and reductive electropolymerisation. The polymers have been characterised by UV-vis absorption spectroscopy and cyclic voltammetry. Possible processes involved in the polymerisation and the structure of the film are discussed.

Introduction

Electroactive polymers are of great interest due to their applications in for example electrocatalysis,[1] electronic devices,[2,3] electrochromics,[4] size-selective membranes,[5] and solar energy conversion.[6] Lately, much interest has been devoted to conducting organic polymers, and to materials consisting of a conjugated polymer linked to redox active metal centres.[7–9] The conjugated backbones of the latter materials may serve to increase the electronic coupling between the metal centres and thus the electron transport rate through the polymer.[7]

Transition metal complexes of bipyridine and related ligands are attractive because of their versatility in terms of how their spectroscopic and chemical properties can be tuned by choice of substituents and metal.[10] Electropolymerisation of such metal complexes may be carried out either oxidatively or reductively depending on the polymerisable ligands. Reductive electropolymerisation of polypyridyl transition metal complexes may be carried out on complexes with a vinyl functionality, according to the route pioneered by Abruna *et al.*[3] The oxidative process has been well studied for ruthenium complexes bearing aromatic amine groups or pendant pyrrole or thiophene groups.[9,11] Also, organic alkoxyaryl-containing molecules have been reported to undergo oxidative coupling to form electronically conducting and redox-active polyphenylene derivatives.[12,13]

We were interested in finding versatile complexes that allow both oxidative and reductive electropolymerisation. In the present paper we report the synthesis and results of the spectroscopic and electrochemical characterisation of ruthenium tris-bipyridyl complexes with methoxystyryl substituents **1**–**4** (Fig. 1). The oxidative and reductive electropolymerisation of these complexes and the properties of the resulting insoluble polymer films are discussed.

Results and discussion

Synthesis

Ligands. A two step synthesis was used to afford the ligands 4-(2-(3-methoxyphenyl)ethenyl)-4′-methyl-2,2′-bipyridine (**7**) and 4,4′-di-(2-(3-methoxyphenyl)ethenyl)-2,2′-bipyridine (**8**). First, nucleophilic addition of the anion of 4,4′-dimethyl-2,2′-bipyridine to *meta*-methoxybenzaldehyde gave the corresponding alcohol.[14] Variation of the proportion of the aldehyde anion allowed us to prepare either the mono-substituted (**5**) or the di-substituted (**6**) bipyridine alcohol. Dehydration was achieved using acetic acid with an easy separation by chromatography for **7** and precipitation in the case of **8** (Scheme 1).

Complexes. The homoleptic complexes tris(4-(2-(3-methoxyphenyl)ethenyl)-4′-methyl-2,2′-bipyridine)ruthenium bis(hexafluorophosphate) (**1**) and tris(4,4′-di(2-(3-methoxyphenyl)-ethenyl)-2,2′-bipyridine)ruthenium bis(hexafluorophosphate) (**2**) (Fig. 1) were obtained by refluxing three equivalents of the desired ligand (**7** or **8**) with $RuCl_3$ in a mixture of EtOH and water (Scheme 2). The complexes precipitated from water solution when the chloride counter ions were exchanged to hexafluorophosphates. The heteroleptic complexes bis-(2,2′-bipyridyl)(4-(2-(3-methoxyphenyl)ethenyl)-4′-methyl-2,2′-bipyridine)ruthenium bis(hexafluorophosphate) (**3**) and bis-(2,2′-bipyridyl)(4,4′-di(2-(3-methoxyphenyl)ethenyl)-2,2′-bipyridine)ruthenium bis(hexafluorophosphate) (**4**) (Fig. 1) were prepared by treating the desired ligand (**7** or **8**, respectively) with one equivalent of $[Ru(bpy)_2Cl_2]$ in a 1 : 1 mixture of EtOH and water, followed by exchange of the chloride counter ions to hexafluorophosphates (Scheme 3).[15]

Spectroscopic characterisation of complexes

Absorption spectroscopy. As expected for ruthenium tris-bipyridyl complexes, the absorption spectra show a broad visible absorbance band centred at 450–480 nm corresponding to a metal-to-ligand charge transfer (MLCT).[10a] The intense bands in the UV region are assigned to two low-lying ligand centred (LC) $\pi \longrightarrow \pi^*$ transitions.[16] The red-shift observed for the MLCT maximum in the visible region (Table 1 and Fig. 2), as compared to the MLCT maximum of $Ru(bpy)_3$, is related to the extent of conjugation of the ligands in the complexes.[16,17] Fig. 2 shows the spectra of **2** and **4** in CH_3CN. The ratio of the values of the absorption coefficients of the two ligand centred transitions correlates with the number of vinylic linkages (Table

DOI: 10.1039/b008697p

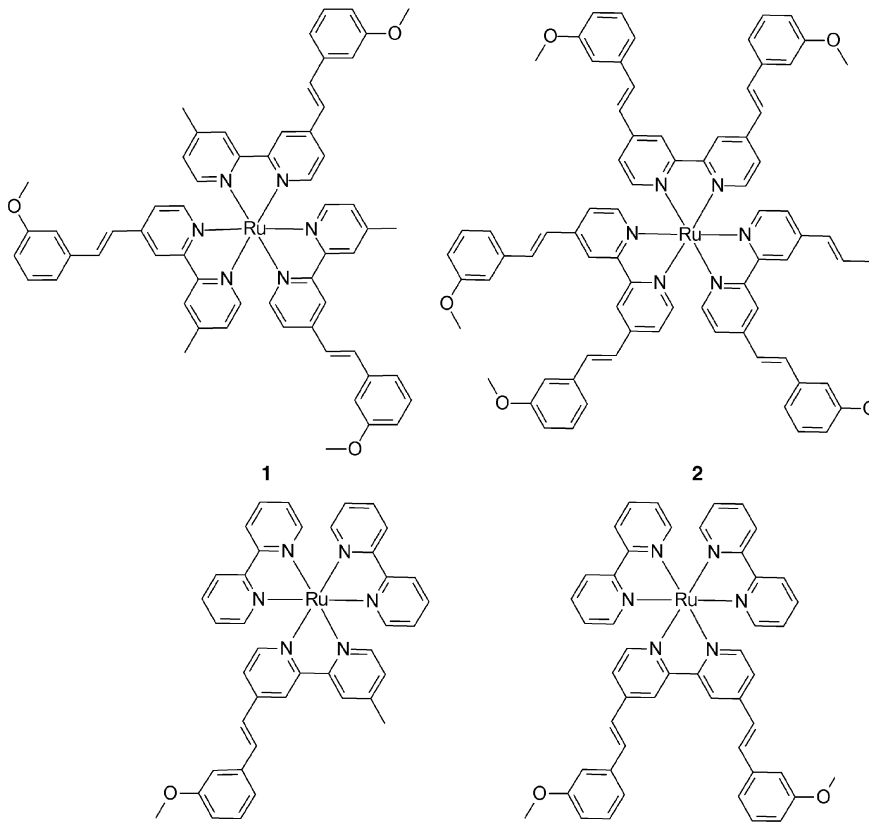

Fig. 1 Complexes investigated in this work.

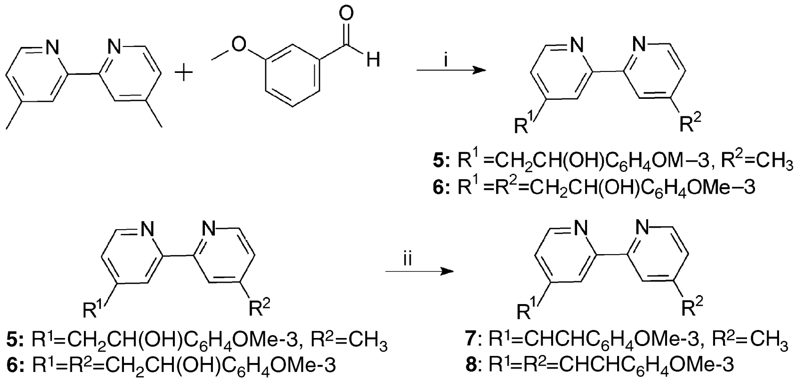

Scheme 1 *Reaction conditions*: (i) 1 equivalent $LiNPr^i_2$, THF, −78 °C, N_2; (ii) conc. AcOH, reflux.

$$3\,L + RuCl_3{\cdot}H_2O \xrightarrow{(i)} [Ru(L)_3]^{2+}\,2PF_6^-$$

Scheme 2 *Reaction conditions*: (i) (a) 1 : 1 EtOH–water, N_2, reflux; (b) NH_4PF_6.

$$L + [Ru(bpy)_2Cl_2] \xrightarrow{(i)} [Ru(bpy)_2L]^{2+}\,2PF_6^-$$

Scheme 3 *Reaction conditions*: (i) (a) complex **3** or **4**, 1 : 1 EtOH–water, N_2, reflux; (b) NH_4PF_6.

1). The absorption coefficient of the MLCT band increases with the number of mono- and di-substituted ligands. The methoxystyryl groups are electron rich and make the ligand strongly electron donating. This stabilises Ru^{III} with respect to Ru^{II} and shifts the HOMO to higher energy.[18]

Electrochemistry and electropolymerisation of complexes

In order to assess the effects of substitution on the formal potentials of complexes **1**–**4**, cyclic voltammograms of their CH_3CN solutions were recorded. The formal potentials for the $Ru^{2+/3+}$ couple of **1** and **2** are 0.74 and 0.84 V for **3** (Fig. 3) and

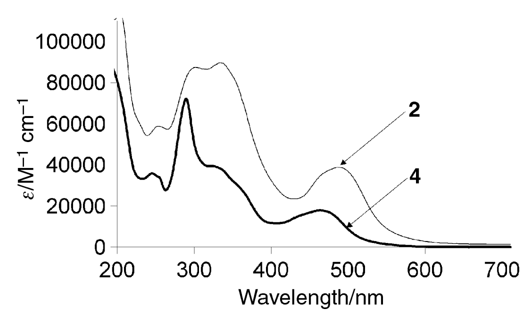

Fig. 2 Absorption spectrum for complexes **2** and **4** in CH_3CN. The instrument resolution is ±2 nm.

4. The formal potentials were calculated from the average of the oxidation and reduction peak potentials. Both oxidation of the metal and of the ligand are diffusion-controlled processes, as seen by the identical slopes and shifts in peak potentials in the plots of peak current upon oxidation as a function of (scan rate)$^{1/2}$ (inset in Fig. 3).[13] The methyl and the methoxystyryl units are electron-donating substituents, and have a lowering

Table 1 Optical properties (maxima values) of complexes **1**–**4** in CH_3CN

Complex	λ_{abs}[a]/nm (10^{-4} ε/M^{-1} cm^{-1}) MLCT	π–π^*_1[b]	π–π^*_2[c]	Emission max. (nm)
1	474 (3.23)	287 (10.2)	334 (6.20)	668
2	489 (3.88)	302 (8.75)	334 (8.97)	673
3	457 (1.48)	287 (6.73)	319 (2.00)	617
4	465 (1.78)	289 (7.21)	313 (4.00)	661

[a] Resolution: ±2 nm. [b] The first ligand centred absorption band. [c] The second ligand-centred absorption band.

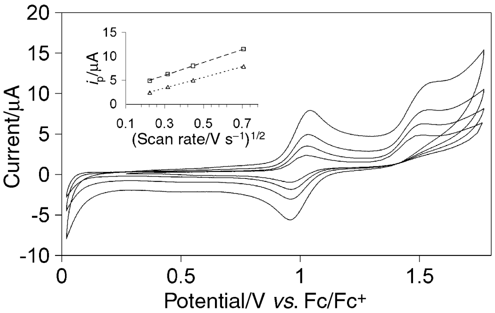

Fig. 3 Cyclic voltammetry of complex **3** in a CH_2Cl_2–TFA–TFAA (8 : 1 : 1) + 0.1 M NBu_4BF_4 solution. TFA/TFAA was added to take care of residual water. The scan rates from top to bottom are 500, 200, 100, 50 mV s^{-1}. The inset is a plot of the anodic peak current (not corrected for background current) of the metal- (△) and ligand-centred (□) oxidations *versus* the square root of the scan rate. TFA = Trifluoroacetic acid, TFAA = trifluoroacetic anhydride.

effect on the formal potential of the ruthenium centre with respect to that of $[Ru(bpy)_3]^{2+}$.[18] The fact that the formal potential of the complexes only changes with the total number of substituents and appears unaffected by the type of substituent (methoxystyryl or methyl) indicates that the electron donating effects of the two substituents are similar in magnitude.

Oxidative electropolymerisation. The oxidative polymerisation of complexes **1**, **2** and **4** was successfully carried out on platinum, gold, glassy carbon and FTO (fluorine doped tin oxide) electrodes. The films were characterised by cyclic voltammetry and absorption spectroscopy (see below). For **3**, not even repeated scanning (>40) at 100 mV s^{-1} through both metal- and ligand-centred oxidations led to any significant change in the voltammetric response, indicating that no polymer film is formed on the electrode surface during the experiment. We thus conclude that the complex must carry at least two polymerisable groups for polymerisation to occur.

Upon oxidation of the methoxystyryl-containing ligands a cation radical is formed. According to the literature, this is located mainly on the phenyl ring of the methoxystyryl group.[19] The cation radical can undergo radical–radical coupling to form dimers linked through aromatic carbons, and possibly also through the carbons belonging to the vinyl group.[12] Scanning repeatedly through the potentials of both the metal- and the ligand-centred oxidations of a solution of complex **4** leads to a rapid growth of the $Ru^{2+/3+}$ wave (Fig. 4), indicating the deposition of poly-**4** onto the electrode surface. The increase in current is due to the combined electroactivity of the polymeric film building up on the electrode surface while monomers are diffusing towards the electrode from the bulk of the solution. During deposition the shape of the voltammogram changes from the typical shape of a diffusing species into the bell-shaped voltammogram of a surface-confined species since for each scan the current will to an increasing proportion be due to the oxidation and reduction of surface-confined material. Upon removal of the electrode from the solution a smooth adherent orange film is observed. The film did not dissolve upon storage of the electrode for hours in dichloromethane or acetonitrile.

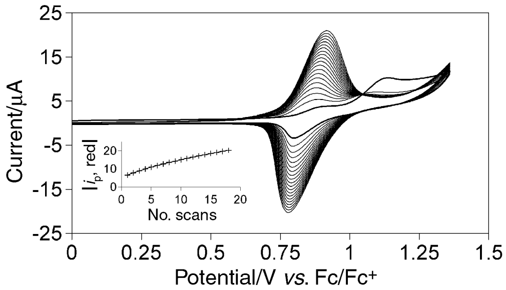

Fig. 4 Oxidative electropolymerisation of complex **4** from a 0.37 mM solution of the complex in CH_2Cl_2 onto a platinum electrode. The scan rate is 100 mV s^{-1}. The initial scan direction is positive. The thick line indicates the first scan. The inset is a plot of the cathodic peak current i_p *vs.* the number of polymerisation scans.

The increase of the peak current (inset, Fig. 4) with number of scans is related to the rate of growth of the polymer film. The rate decreases somewhat after the initial three to four scans, but growth continues up to at least 20 scans. 20 scans at 100 mV s^{-1} result in a film of poly-**4** with an apparent surface coverage of about 2×10^{-9} mol cm^{-2}.† Roughly the same behaviour is observed for the electrochemical deposition of poly-**1** and poly-**2**, but a larger increase in surface coverage per deposition scan is observed. The electropolymerisation rate increases with the number of polymerisable groups and films of poly-**1** and poly-**2** were deposited to apparent surface coverage above 2×10^{-8} mol cm^{-2} (≈200 monolayers). When oxidative electropolymerisation was carried out with the counter electrode kept in the same compartment as the working electrode polymer film formation was observed also at the counter electrode, where the converse reaction takes place.

Electron transport through the polymer film takes place by successive electron transfer between neighbouring redox centres. The redox reactions are accompanied by uptake (or expulsion) of counter ions to maintain electroneutrality. It remains unclear where the film growth takes place, at the polymer film/electrolyte (i) or at the electrode/polymer film interface (ii). Neither seems to be favoured: for (i), ruthenium(III) centres at the surface would have to oxidise methoxystyryl units, which according to our electrochemical experiments should not occur; and for (ii), cationic monomers would have to diffuse through the polycation network of the already formed polymer film.

Reductive electropolymerisation. It has been shown that vinylic linkages in styryl- and dimethoxystyryl-bipyridine ligands of ruthenium tris-bipyridyl complexes are activated towards polymerisation upon electrochemical reduction of the ligands.[20,21] The polymerisation is believed to proceed *via* several pathways, of which the radical–radical hydrodimerisation pathway, leading to butyl-bridged complexes, is thought to be the most important.[22,23] The methoxystyryl ligands of the complexes studied here also undergo coupling upon electroreduction. Reduction of **1**, **2**, **3** and **4** shows three ligand reduc-

---

† (a) The apparent surface coverages (Γ) were calculated using the equation $\Gamma = Q_{red}/nFA$, where Q_{red} is the integrated charge under the re-reduction wave of the metal centre recorded at a scan rate where the film exhibited a surface confined behaviour, *n* the number of electrons transferred, *F* Faraday's constant, and *A* the projected area of the electrode. Statements about the apparent number of "monolayers" of polymeric material are based on a hard-sphere model for $[Ru(bpy)_3]^{2+}$ type complexes, in which a monolayer corresponds to roughly 1×10^{-10} mol cm^{-2}. Since the complexes studied here are significantly larger than $Ru(bpy)_3$, the actual number of molecular layers in the films will be somewhat larger. (b) See ref. 7(*a*) and references therein.

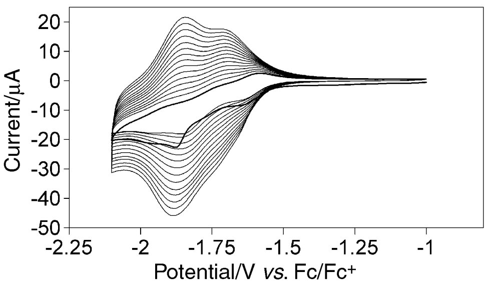

Fig. 5 Cyclic voltammograms recorded continuously at a 100 mV s^{-1} in a solution of complex **1** in acetonitrile. The scan rate is 100 mV s^{-1} and the scans were initiated at -1.0 V. The thick line indicates the first scan.

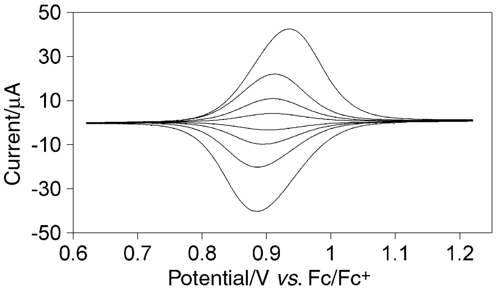

Fig. 6 Cyclic voltammetry at different scan rates of a film of oxidatively deposited poly-**4** in complex-free electrolyte. The apparent surface coverage is $\approx 2 \times 10^{-9}$ mol cm^{-2} which is equal to about 20 monolayers. The scan rates, from top to bottom, are 200, 100, 50 and 20 mV s^{-1}. The initial scan direction was positive.

tions in the interval -1.5 to -2.2 V. Sweeping the potential repeatedly through two or all three ligand-based reductions of **1** leads to the formation of an adherent orange electroactive film on the electrode surface. Cyclic voltammograms recorded during the reductive deposition of poly-**1** onto a platinum electrode are shown in Fig. 5. Also **2** and **4** undergo reductive electropolymerisation, but no polymer film is formed of **3**.

Characterisation of the polymers

Electrochemistry. In Fig. 6 cyclic voltammograms of oxidatively deposited poly-**4** (poly-**4**-*ox*) in complex-free electrolyte are shown. The film of poly-**4**-*ox* displays one metal centred oxidation and gives a surface wave type response up to 100 mV s^{-1} with a peak separation of approximately 10 mV and a full width at half-maximum (FWHM) of 120 mV.[24]

At higher scan rates the voltammetric response of the polymer film changes from the surface-confined thin film behaviour to a response characteristic of semi-infinite diffusion conditions. This occurs at scan rates where not all the metal centres in the film are oxidised during one scan. The redox reactions in the polymer films are accompanied by migration of counter ions to maintain electroneutrality. Also solvent can be transferred and polymer configurational changes can occur. It is common that the overall electron transport rate is governed by the counter ion migration rate.[1]

Films of reductively deposited poly-**1** (poly-**1**-*red*) exhibit similar electrochemical properties to those of poly-**1**-*ox*, except for a large irreversible wave slightly positive of the Ru$^{2+/3+}$ wave observed in the first anodic scan. This is likely due to oxidation of unchanged methoxy-phenyl units in the film.[21] The formal potentials of poly-**1**-*ox* and poly-**1**-*red* films are within 50 mV of each other. The electrochemical stability of poly-**1**-*red* and poly-**1**-*ox* is largely dependent on the potential limits of the experiment. Both polymers are stable during extensive cycling of the potential within ±0.20 V of $E^{\circ\prime}$(Ru$^{2+/3+}$). Extending the potential window to ± 0.50 V leads to losses of 10–30% of the initial electroactivity over 50 scans at a 100 mV s^{-1}, but variations between the electrodes were large and no signs of greater electrochemical stability of poly-**1**-*red* than poly-**1**-*ox* was observed.

Table 2 MLCT maximum for complexes **1** and **2** in solution and in polymer films

Complex	λ_{max}^{sol}/nm	λ_{max}^{poly}/nm		$\Delta\lambda = \lambda_{max}^{sol} - \lambda_{max}^{poly}$	
		Oxidative	Reductive	Oxidative	Reductive
1	475	461	467	14	8
2	485	469	n.d.	16	n.d.

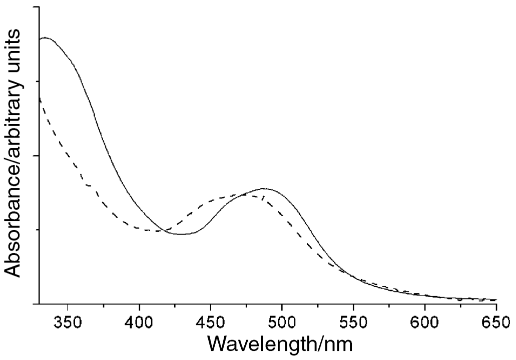

Fig. 7 UV-Vis absorption spectra of complex **2** dissolved in acetonitrile (plain) and poly-**2**-*ox* on FTO measured in a cell filled with acetonitrile (dashed). The absorption spectrum of **2** was referenced to a solvent blank and the FTO/poly-**2**-*ox* spectrum was referenced to a blank FTO electrode in solvent.

Absorption spectroscopy. Red-shifts of the MLCT maximum of ruthenium complexes with large conjugated ligands with respect to the complexes [Ru(bpy)$_3$]$^{2+}$ and [Ru(dmbpy)$_3$]$^{2+}$, where dmbpy is 4,4′-dimethyl-2,2′-bipyridine, have been reported.[10a,b] This is observed for our complexes (Fig. 2, Table 1) in solution. Binuclear ruthenium polypyridyl complexes bridged by a conjugated vinyl or a divinylphenyl unit have been shown to have significantly red-shifted MLCT maxima compared to that of the corresponding mononuclear complex.[17,26] However, only blue-shifts of the MLCT maxima of the deposited polymers were observed, regardless of the deposition method (Table 2, Fig. 7), suggesting that the conjugated systems in the ligands are not as extended in the polymer films as in an unchanged complex in solution. This is as expected for the reductively prepared polymer, but surprising in the case of the oxidatively prepared polymers.[12b,c,13] According to the literature, the consumption of vinylic linkages during polymerisation of transition metal complexes of 4-methyl-4′-vinylbipyridine leads to a decreased extent of conjugation for the ligands and consequently a blue-shift of the MLCT maximum.[10b] The blue-shift observed for our oxidatively prepared polymers is likely due to the presence of similar saturated links between the complexes as when the reductive route is employed. As the shift is larger for poly-*ox* films than for poly-*red* ones, the vinyl consumption is probably higher during oxidative polymerisation.

Stability tests. In an attempt to dissolve the oxidatively and reductively formed films of poly-**1**, and to explore the chemical stability of the polymer films, polymer films on FTO were soaked and left standing in toluene, pyridine, dimethyl sulfoxide (DMSO) or dimethylformamide (DMF) during ten days, after which absorption spectra of the electrodes were recorded. The stability of the films in DMSO and DMF were significantly higher for the reductively deposited films. For instance, in DMF, 97% of the initial absorbance remained after ten days for poly-**1**-*red* whereas for poly-**1**-*ox* only 76% remained. The films were also left standing for up to 18 hours in neutral and basic water, MeOH or EtOH. Also in these experiments, poly-**1**-*ox* proved less stable than poly-**1**-*red*. The stability of poly-**1**-*ox* in pure water was poor with a 10% loss of absorbance over 18 hours whereas no significant loss of absorbance was detected for poly-**1**-*red* in water. In 0.1 M NaOH water solution the differences in stability of poly-**1**-*red* and poly-**1**-*ox* are even more pronounced, with an almost complete loss of absorbance of poly-**1**-*ox* but no significant loss at all of poly-**1**-*red*.

Conclusion

Bipyridine ligands with methoxystyryl units that can be activated towards electropolymerisation both at positive and negative potentials (capable of both oxidative and reductive polymerisation) have been prepared and their ruthenium complexes synthesized. Two polymerisable groups on the same complex are necessary for the formation of an insoluble polymeric film on an electrode surface. Oxidative electropolymerisation was carried out in CH_2Cl_2 and reductive electropolymerisation in CH_3CN. It was possible to deposit relatively thick (≈200 layers of complex) polymer films by oxidative deposition. The spectroscopic measurements indicate a lower degree of conjugation of the complexes in the oxidatively deposited film compared to that of the unchanged monomer in solution. This is pointing towards a coupling, which, to a large extent involves the carbon atoms belonging to the vinyl groups.

Experimental

Materials

All reagents were from commercial sources used without further purification. Solvents were HPLC grade used without further purification with the following exceptions: acetonitrile (CH_3CN) was purchased (Aldrich) anhydrous and further dried statically for several weeks over 3 Å molecular sieves previously regenerated by heating to 350 °C under vacuum for 48 hours; tetrahydrofuran (THF) was distilled from sodium; and diisopropylamine (DIPA), triethylamine (Et_3N) and dichloromethane (CH_2Cl_2) were distilled from CaH_2. Butyllithium (BuLi) was stored in a desiccator under argon, and used as fresh (no precipitate) 1.6 M solutions in hexane. Trifluoroacetic acid and trifluoroacetic acid anhydride were stored at -18 °C and used as received. Ferrocene was purified by sublimation and tetrabutylammonium tetrafluoroborate was dried under vacuum at 140 °C for 48 hours. Syntheses were performed under a nitrogen atmosphere. Column chromatography was performed with Merck silica gel (230–400 mesh). Thin-layer chromatography (TLC) was run on Merck precoated silica gel 60-F_{254} plates. Transparent conducting oxide electrodes of fluorine-doped tin oxide on a 3 mm glass support (sheet resistance 8 Ω) were purchased from Liffey-Owens-Ford. Elemental analyses were performed by Analytische Laboratorien, Lindlar, Germany.

Physical characterisation

NMR spectra (^1H at 400 MHz and ^{13}C at 100 MHz) were recorded on a Varian Unity 400 spectrometer for $CDCl_3$ solutions unless otherwise stated. The chloroform signals at δ 7.26 (for ^1H) or 77.0 (for ^{13}C) were used as indirect reference to TMS. UV–Vis absorption spectra were recorded using a Hewlett-Packard 8453 diode-array spectrophotometer and referenced against a solvent blank (CH_3CN). The fluorine-doped tin oxide electrodes with polymer films deposited on the surface were positioned against the wall of a 1 cm quartz cuvette containing CH_3CN. Emission spectroscopy measurements were performed with a Spex Fluorolog Model 212 spectrometer with photon counting detection. The emission was monitored at right angles with respect to the excitation. The MLCT absorption maximum of the respective complex was chosen as excitation wavelength. The samples were diluted until the absorbance at the maximum of the metal-to-ligand charge-transfer band was approximately 0.1.

Electrochemistry

Electrochemical experiments were performed using an ECO Chemie Autolab PGSTAT 10 potentiostat and a three-electrode system. Potentials are quoted with respect to the ferrocene redox couple unless otherwise noted. All electrochemical experiments were performed inside an argon filled drybox at room temperature unless otherwise noted. The supporting electrolyte in all experiments was 0.1 M NBu_4BF_4. The counter electrode was a coiled platinum wire kept in a separate compartment fitted with a ceramic frit. The reference for measurements in acetonitrile was an Ag–0.01 M $AgNO_3$ + 0.1 M NBu_4BF_4 electrode, separated from the solution with an 8 cm salt bridge filled with electrolyte and fitted with a ceramic frit. The potential of this electrode was -0.08 V *vs.* the ferrocene couple (+0.24 V *vs.* SCE).[25] A silver wire was used as quasi-reference in all experiments carried out in dichloromethane; its potential was measured *versus* the ferrocene couple after experiments. Working electrodes of gold, platinum and glassy carbon shrouded in Kel-F were employed. The diameters of the electrodes were 2 mm except for the glassy carbon electrodes which had a diameter of 4 mm. The electrodes were polished in an aqueous suspension of 0.3 μm diameter alumina particles (Buehler) on a polishing cloth (Buehler), sonicated in water (deionised to a resistivity of 18 MΩ using a Millipore purification pak) for at least 15 min to remove alumina particles followed by 15 min sonication in dichloromethane to remove organic impurities. The electrodes were then taken into the drybox. Transparent conducting oxide electrodes were cut from large FTO sheets into 10 × 25 mm pieces. The FTO electrodes were pre-treated by sonication in acetone for at least 10 min, rinsed under a stream of millipore water (0.1–0.5 L) and then heated to 400 °C in a stream of air for 30 min. The electrodes were taken into the drybox while still warm (>100 °C). Glassware was heated to ≥110 °C overnight and brought into the drybox while still warm. All electropolymerisation was carried out in dilute (0.3–1 mM) solutions of the complexes at scan rates of 50–100 mV s^{-1}. Reductive electropolymerisation was carried out in CH_3CN by scanning the potential through at least two of the three ligands reductions (all in the region -1.5 to -2.2 V *vs.* ferrocene). All oxidative electropolymerisation was carried out in CH_2Cl_2 or CH_2Cl_2–TFA–TFAA (8 : 1 : 1) mixtures. The TFAA–TFA was added to the mixture to take care of residual water.

Synthesis

Substituted 4,4′-dimethyl-2,2′-bipyridines 5 and 6. Lithium diisopropylamide was formed by mixing BuLi (2.48×10^{-3} mol for monodeprotonation (**5**) and 5.92×10^{-3} mol for bis-deprotonation (**6**)) with DIPA (0.39 mL for monodeprotonation and 0.78 mL for bis-deprotonation) in 20 mL THF at -60 °C under N_2. The $LiNPr^i_2$ solution was stirred at room temperature for 30 minutes and cooled to -40 °C. 4,4′-Dimethyl-2,2′-bipyridine (0.5 g, 2.48×10^{-3} mol) dissolved in 20 mL THF was added to the $LiNPr^i_2$ through a double tipped needle, the cooling bath removed and the black reaction mixture then stirred at room temperature during one hour. After cooling to -60 °C a solution of 3-methoxybenzaldehyde (0.727 mL, 2.48×10^{-3} mol) in 10 mL THF was added through a double tipped needle. A yellow precipitate was formed. Stirring was continued for three hours, then the mixture was stirred into water and extracted with CH_2Cl_2 (1 × 100 mL). The organic phase was washed with brine (150 mL), dried over $MgSO_4$ and concentrated.

*4-(2-Hydroxy-2-(3-methoxyphenyl)ethyl)-4-methyl-2,2′-bipyridine (**5**).* The crude product was chromatographed using ethyl acetate–pentane–Et_3N (50 : 48 : 2) to give compound **5** in 46% yield (0.364 g, 1.14×10^{-3} mol). ^1H NMR ($CDCl_3$): δ 8.54 (1H, $J = 5.2$, d, pyridine), 8.51 (1H, $J = 5.2$, d, pyridine), 8.31 (1H, s, pyridine), 8.21 (1H, s, pyridine), 7.25 (1H, t, $J = 8$ Hz, methoxyphenyl), 7.12 (2H, m, pyridine + methoxyphenyl), 6.94 (2H, m, pyridine + methoxyphenyl), 6.82 (1H, dd, $J_1 = 8$, $J_2 = 2.4$ Hz, methoxyphenyl), 4.99 (1H, m, benzylic C*H*(OH)), 3.93 (3H, s, benzylic CH_3), 3.08 (2H, m, benzylic CH_2) and 2.43 (3H, s, OCH_3). ^{13}C NMR: δ 160.0, 156.2, 156.0, 149.2, 149.1, 148.7, 148.5, 145.6, 129.8, 125.2, 125.0, 122.3, 122.2, 118.3, 113.7, 111.4, 74.6, 55.5, 45.6 and 21.4.

*4,4′-Di(2-hydroxy-2-(3-methoxyphenyl)ethyl)-2,2′-bipyridine (**6**).* NMR of the crude product showed more than 85% of conversion compared to the aldehyde and complete conversion compared to the bipyridine. The crude product **6** was used without further purification. ^1H NMR (200 MHz) ($CDCl_3$): δ 8.37 (2H, d, $J = 5$, pyridine), 8.21 (2H, broad s, pyridine), 7.24 (2H, t, $J = 8.4$, methoxyphenyl), 7.06 (2H, dd, $J_1 = 5$, $J_2 = 1.6$ Hz, methoxyphenyl), 6.93 (4H, m, methoxyphenyl), 6.80 (2H, m, pyridine), 4.98 (2H, m, benzylic C*H*(OH)), 3.77 (6H, s, OCH_3) and 3.03 (4H, m, benzylic CH_2). ^{13}C NMR: δ 159.7, 155.6, 148.9, 148.8, 145.4, 129.5, 125.0, 122.2, 118.1, 113.3, 111.1, 74.2, 55.2 and 45.5.

4-(2-(3-Methoxyphenyl)ethenyl)-4′-methyl-2,2′-bipyridine (7). Compound **5** (0.367 g, 1.14×10^{-3} mol) was dissolved in conc. AcOH (5 mL, excess) and stirred under reflux during 18 hours. The reaction mixture was poured into sat. aq. $NaHCO_3$ (100 mL) and extracted with CH_2Cl_2 (100 mL), dried over $MgSO_4$ and concentrated to give **7** in 74% yield (0.255 g, 0.84×10^{-3} mol) from **5** and 34% yield from 4,4′-dimethyl-2,2′-bipyridine. ^1H NMR ($CDCl_3$): δ 8.637 (1H, d, $J = 5.2$, pyridine), 8.57 (1H, d, $J = 4.8$, pyridine), 8.51 (1H, d, $J = 1.2$, pyridine), 8.26 (1H, broad s, pyridine), 7.42 (1H, d, $J = 16.4$, vinylic), 7.37 (1H, dd, $J_1 = 5.2$, $J_2 = 1.2$, pyridine), 7.31 (1H, t, $J = 8$, methoxyphenyl), 7.16 (2H, m, methoxyphenyl + pyridine), 7.11 (2H, m, vinylic + methoxyphenyl), 6.88 (1H, dd, $J_1 = 8$, $J_2 = 2.4$ Hz, methoxyphenyl), 3.86 (s, 3H, OCH_3) and 2.45 (s, 3H, CH_3). ^{13}C NMR: δ 160.2, 156.8, 156.0, 149.7, 149.1, 148.5, 137.9, 133.5, 130.0, 126.7, 125.1, 122.3, 121.2, 120.0, 118.6, 114.7, 112.4, 55.5 and 21.5. Calc. for $C_{28}H_{18}N_2O$: C, 79.44; H, 6.00; N, 9.26. Found: C, 78.24; H, 6.17; N, 9.63%.

4,4′-Di(2-(3-methoxyphenyl)ethenyl)-2,2′-bipyridine (8). Crude compound **6** was dissolved in conc. AcOH (10 mL, excess) and the mixture stirred under reflux for 18 hours. When the reaction mixture was cooled to room temperature the product precipitated and **6** was obtained with a yield of 36% (0.378 g, 0.898×10^{-3} mol) from 4,4′-dimethyl-2,2′-bipyridine. ^1H NMR ($CDCl_3$): δ 8.69 (2H, d, $J = 4.8$, pyridine), 8.61 (2H, s, pyridine), 7.47 (2H, $J = 16.4$, d, vinylic), 7.43 (2H, d, $J = 4.8$, pyridine), 7.32 (2H, t, $J = 7.6$ Hz, methoxyphenyl), 7.18 (2H, d, methoxyphenyl), 7.14 (4H, m, vinylic + methoxyphenyl), 6.90 (2H, m, pyridine) and 3.87 (s, 6H, OCH_3). ^{13}C NMR: δ 149.5, 148.9, 133.3, 129.8, 126.4, 124.9, 122.2, 121.1, 119.7, 118.4, 114.5, 112.1, 55.3 and 21.2. IR (KBr): 3306, 2937, 1598, 1487, 1462, 1435, 1263, 1149, 1046, 783 and 700 cm^{-1}. Calc. for $C_{14}H_{12}NO$: C, 79.98; H, 5.75; N, 6.66. Found: C, 79.11; H, 5.81; N, 6.56%.

Homoleptic complexes. $RuCl_3 \cdot xH_2O$ (48 mg, 0.23×10^{-3} mol) and compound **7** or **8** (0.69×10^{-3} mol) were stirred at reflux in a 20 mL mixture of EtOH and water (1 : 1) under nitrogen for 24 hours during which time the solution turned dark red. The EtOH was distilled off and a solution of NH_4PF_6 (1.24 g, 7.66×10^{-3} mol) in water (25 mL) added, after which an orange-brown precipitate appeared. The precipitate was filtered off, washed with water (100 mL) and diethyl ether (100 mL). The product was dried under reduced pressure during 24 h.

*Tris(4-(2-(3-methoxyphenyl)ethenyl)-4′-methyl-2,2′-bipyridine)ruthenium bis(hexafluorophosphate) (**1**).* 37% yield (0.111 g, 85.5×10^{-6} mol). ^1H NMR ($CDCl_3$): δ 8.97 (3H, pyridine), 8.76 (3H, d, pyridine), 8.04–7.67 (12H, m, methoxyphenyl), 7.43–7.34 (15 H, m, methoxyphenyl), 7.26 (3H, m, methoxyphenyl), 6.94 (3H, m, methoxyphenyl), 3.84 (9H, s, OCH_3) and 2.59 (s, 9H, CH_3). Calc. for $C_{60}H_{54}F_{12}N_6O_3P_2Ru$: C, 55.52; H, 4.19; N, 6.47. Found: C, 55.83; H, 4.69; N, 6.14%.

*Tris(4,4′-di(2-(3-methoxyphenyl)ethenyl)-2,2′-bipyridine)ruthenium bis(hexafluorophosphate) (**2**).* Compound **2** was obtained in 41% yield (0.147 g, 86.9×10^{-6} mol). ^1H NMR ($CDCl_3$): δ 9.15 (6H, m, pyridine), 8.10 (6H, d, $J = 6.4$, pyridine), 7.83 (6H, d, $J = 16.4$, vinylic), 7.54 (6H, d, $J = 6$, pyridine), 7.46 (6H, d, $J = 16.4$, vinylic), 7.37 (12H, m, methoxyphenyl), 7.27 (12H, m, methoxyphenyl), 6.99 (6H, dd, $J_1 = 7.6$, $J_2 = 1.6$ Hz, methoxyphenyl) and 3.86 (18H, s, OCH_3). ^{13}C NMR: δ 160.5, 157.7, 151.7, 147.0, 137.6, 136.8, 130.2, 124.7, 121.3, 120.4, 115.5, 112.6 and 55.0. Calc. for $C_{84}H_{72}F_{12}N_6O_6P_2Ru$: C, 61.05; H, 4.39; N, 5.09. Found: C, 60.78; H, 4.65; N, 4.92%.

Heteroleptic complexes. *Bis(2,2′-bipyridyl)(4-(2-(3-methoxyphenyl)ethenyl)-4′-methyl-2,2′-bipyridine)ruthenium bis(hexafluorophosphate) (**3**).* $[Ru(bpy)_2Cl_2]$[14] (0.035 g, 66×10^{-6} mol) and compound **7** (20 mg, 66×10^{-6} mol) were stirred at reflux in a 10 mL mixture of EtOH and water (1 : 1), under argon for one hour. The solution turned deep red. The EtOH was distilled off and a solution of NH_4PF_6 (0.215 g, 1.32×10^{-3} mol) in water (15 mL) added and stirred overnight (18 h), after which time an orange precipitate had appeared. The precipitate was filtered off and dried under vacuum overnight to give **3** in 94% yield (0.063 g, 62.5×10^{-6} mol). ^1H NMR (acetone): δ 9.00 (1H, s, substituted pyridine), 8.84–8.78 (4H, m, non-substituted bipyridines), 8.70 (1H, s, substituted pyridine), 8.22–8.16 (5H, m, 4H non-substituted bipyridines + 1H substituted bipyridines), 8.09–8.04 (5H, m, non-substituted bipyridines + 1H substituted bipyridines), 7.94 (1H, d, $J = 5.6$, substituted pyridine), 7.77 (1H, d, $J = 16$, vinylic), 7.67 (1H, m, substituted pyridine), 7.59 (4H, m, non-substituted bipyridines), 7.42 (1H, d, $J = 16$ Hz, vinylic), 7.36 (1H, m, methoxyphenyl), 7.23 (2H, m, methoxyphenyl), 6.98 (1H, m, methoxyphenyl), 3.85 (3H, s, OCH_3), 2.57 (3H, s, py CH_3). Calc. for $C_{40}H_{34}F_{12}N_6OP_2Ru \cdot 7H_2O$: C, 42.45; H, 4.27; N, 7.42. Found: C, 41.86; H, 3.79; N, 8.00%.

*Bis(2,2′-bipyridyl)(4,4′-di(2-(3-methoxyphenyl)ethenyl)-2,2′-bipyridine)ruthenium bis(hexafluorophosphate) (**4**).* $[Ru(bpy)_2Cl_2]$[14] (0.025 g, 47.5×10^{-6} mol) and compound **8** (0.020 g, 66×10^{-6} mol) were stirred at reflux in a 10 mL mixture of EtOH and water (1 : 1), under argon for one hour. The solution turned deep red. The EtOH was distilled off and a solution of NH_4PF_6 (0.080 g, 0.48×10^{-3} mol) in water (10 mL) added and stirred overnight (18 h), after which time an orange precipitate had appeared. The precipitate was filtered off and dried under vacuum overnight to afford **4** in 46% yield (0.024 g, 22.3×10^{-6} mol). ^1H NMR (acetone): δ 9.08 (2H, s, substituted pyridine), 8.84 (4H, d, $J = 8.4$, non-substituted bipyridines), 8.23 (4H, t, $J = 8$, non-substituted bipyridines), 8.19 (2H, d, $J = 5.6$, methoxyphenyl), 8.08 (2H, d, $J = 5.6$, substituted pyridine), 7.96 (2H, d, $J = 6$, methoxyphenyl), 7.79 (2H, d, $J = 16$, vinylic), 7.71 (2H, d, $J = 6$, substituted pyridine), 7.61 (4H, m, non-substituted bipyridines), 7.45 (2H, d, $J = 16$ Hz, vinylic), 7.37 (2H, m, methoxyphenyl), 7.27 (4H, m, non-substituted bipyridines), 6.98 (2H, m, methoxyphenyl) and 3.86 (6H, s, OCH_3). Calc. for $C_{48}H_{40}F_{12}N_6O_2P_2Ru \cdot 2Et_2O$: C, 52.87; H, 4.75; N, 6.61. Found: C, 53.74; H, 4.46; N, 6.77%.

Acknowledgements

The Swedish Research Council for Engineering Sciences (TFR), the Foundation for strategic environmental research (MISTRA), and the Swedish Natural Science Research Council (NFR) are acknowledged for financial support.

References

1 C. P. Andrieux and J.-M. Savéant, *Molecular Design of Electrode Surfaces*, Wiley-Interscience, New York, 1992, vol. 22 and references therein; M. E. G. Lyons, *Electroactive Polymer Electrochemistry: Part 1—Fundamentals*, 2nd edn., Plenum Press, New York, 1994 and references therein.

2 P. Denisevich, K. W. Willman and R. W. Murray, *J. Am. Chem. Soc.*, 1981, **103**, 4727.

3 H. D. Abruna, P. Denisevich, M. Umana, T. J. Meyer and R. W. Murray, *J. Am. Chem. Soc.*, 1981, **103**, 1.

4 P. M. S. Monk, R. J. Mortimer and D. R. Rosseinsky, *Electrochromism: Fundamentals and Applications*, VCH, Weinheim, 1995.

5 T. Ikeda, R. Schmehl, P. Denisevich, K. Willman and R. W. Murray, *J. Am. Chem. Soc.*, 1982, **104**, 2683; A. G. Ewing, B. J. Feldman and R. W. Murray, *J. Phys. Chem.*, 1985, **89**, 1263; S. Gould, K. H. Gray, R. W. Linton and T. J. Meyer, *J. Phys. Chem.*, 1995, **99**, 16052.

6 H. D. Abruna and A. J. Bard, *J. Am. Chem. Soc.*, 1981, **103**, 6898; J. A. Moss, J. M. Stipkala, J. C. Yang, C. A. Bignozzi, G. J. Meyer, T. J. Meyer, X. Wen and R. W. Linton, *Chem. Mater.*, 1998, **10**, 1748; M. A. Fox and P. F. Britt, *New J. Chem.*, 1992, **16**, 113; E. M. Girotto, W. A. Gazotti and M.-A. De Paoli, *J. Phys. Chem. B*, 2000, **104**, 6124.

7 (*a*) C. G. Cameron and P. G. Pickup, *J. Am. Chem. Soc.*, 1999, **121**, 11773; (*b*) G. Zotti, G. Schiavon, S. Zecchin, A. Berlin, G. Pagani and A. Canavesi, *Synth. Met.*, 1996, **76**, 255.

8 S. S. Zhu and T. M. Swager, *Adv. Mater.*, 1996, **8**, 497; B. J. MacLean and P. G. Pickup, *Chem. Commun.*, 1999, 2471.

9 J. G. Eaves, H. S. Munro and D. Parker, *Inorg. Chem.*, 1987, **26**, 644; J. A. Crayston, A. Iraqi, J. J. Morrison and J. C. Walton, *Synth. Met.*, 1997, **84**, 441; J. Wang and F. R. Keene, *J. Electroanal. Chem.*, 1996, **405**, 71; C. D. Ellis, L. D. Margerum, R. W. Murray and T. J. Meyer, *Inorg. Chem.*, 1983, **22**, 1283.

10 (*a*) A. Juris, V. Balzani, F. Barigelletti, S. Campagna, P. Belser and A. Von Zelewsky, *Coord. Chem. Rev.*, 1988, **84**, 85; (*b*) S. L. Bommarito, S. P. Lowery-Bretz and H. D. Abruna, *Inorg. Chem.*, 1992, **31**, 495; (*c*) C. Kaes, A. Katz and M. W. Hosseini, *Chem. Rev.*, 2000, **100**, 3553.

11 M.-N. C. Dunand-Sauthier, A. Deronzier, J.-C. Moutet and S. Tingry, *J. Chem. Soc., Dalton Trans.*, 1996, 2503.

12 (*a*) L. M. Goldenberg and P. C. Lacaze, *Synth. Met.*, 1993, **58**, 271; (*b*) Rault-Berthelot, M. M. Granger and E. Raoult, *J. Electroanal. Chem.*, 2000, **486**, 40; (*c*) A. Haj Said, C. Dridi, S. Roudesli and F. Matoussi Mhalla, *Eur. Polym. J.*, 2000, **36**, 909; (*d*) B. Fabre, K. Michelet, N. Simonet and J. Simonet, *J. Electronanal. Chem.*, 1997, **425**, 67.

13 A. Haj Said, F. Matoussi Mhalla, C. Amatore and J.-N. Verpeaux, *J. Electroanal. Chem.*, 1999, **464**, 85.

14 B. P. Sullivan, D. J. Salmon and T. J. Meyer, *Inorg. Chem.*, 1978, **17**, 3334.

15 T. A. Heimer, S. T. D'Arcangelis, F. Farzad, J. M. Stipkala and G. J. Meyer, *Inorg. Chem.*, 1996, **35**, 5319.

16 P. D. Beer, O. Kocian, R. J. Mortimer and C. Ridgeway, *J. Chem. Soc., Dalton Trans.*, 1993, 2629.

17 J. R. Shaw, R. T. Webb and R. H. Schmehl, *J. Am. Chem. Soc.*, 1990, **112**, 1117.

18 V. Skarda, M. J. Cook, A. P. Lewis, G. S. G. McAuliffe, A. J. Thomson and D. J. Robbins, *J. Chem. Soc., Perkin Trans. 2*, 1984, 1293.

19 A. J. Bard, *Encyclopedia of Electrochemistry of the Elements*, vol. XI, Marcel Dekker, New York, 1978.

20 C. R. Leidner, B. P. Sullivan, R. A. Reed, B. A. White, M. T. Crimmins, R. W. Murray and T. J. Meyer, *Inorg. Chem.*, 1987, **26**, 882.

21 P. D. Beer, O. Kocian, R. J. Mortimer and C. Ridgeway, *J. Chem. Soc., Faraday Trans.*, 1993, 333.

22 J. M. Calvert, R. H. Schmehl, B. P. Sullivan, J. S. Facci, T. J. Meyer and R. W. Murray, *Inorg. Chem.*, 1983, **22**, 2151.

23 T. F. Guarr and F. C. Anson, *J. Phys. Chem.*, 1987, **91**, 4037.

24 Theoretically, at room temperature, a 0 V peak separation and a 90.6 mV FWHM is expected for a one-electron reaction of an ideal surface-immobilised redox couple experiencing no lateral intermolecular interactions. See for example ref. 25.

25 A. J. Bard and L. R. Faulkner, *Electrochemical Methods: Fundamentals and Applications*, John Wiley & Sons, New York, 1980.

26 S. Boyde, G. F. Strouse, W. E. Jones and T. J. Meyer, *J. Am. Chem. Soc.*, 1990, **112**, 7395.